

# Restrictive Expression of Acid-Sensing Ion Channel 5 (Asic5) in Unipolar Brush Cells of the Vestibulocerebellum

Nina Boiko<sup>1</sup>, Volodymyr Kucher<sup>1</sup>, Bin Wang, James D. Stockand\*

Department of Physiology, University of Texas Health Science Center, San Antonio, Texas, United States of America

## Abstract

Acid-sensing ion channels (Asic) are ligand-gated ion channels in the Degenerin/Epithelial Na<sup>+</sup> channel (Deg/ENaC) family. Asic proteins are richly expressed in mammalian neurons. Mammals express five Asic genes: *Asic1-5*. The gene product of *Asic5* is an orphan member of the family about which little is known. To investigate *Asic5* expression, we created an *Asic5* reporter mouse. We find that *Asic5* is chiefly expressed in the brain in the cerebellum, specifically in the ventral uvula and nodulus of the vestibulocerebellum. Here, *Asic5* is restrictively expressed in a subset of interneurons in the granular layer. The locale, distinctive shape and immunohistochemical properties of these *Asic5*-expressing interneurons identify them as unipolar brush cells (UBC). *Asic5* is richly expressed in a subset of UBCs that also express the metabotropic glutamate receptor 1 $\alpha$  (mGluR1 $\alpha$ ) but not those that express calretinin. Results from single cell RT-PCR and electrophysiological examination of these cells are consistent with this identity. Such observations are consistent with *Asic5* playing a key role in the physiology of UBCs and in the function of the vestibulocerebellum.

**Citation:** Boiko N, Kucher V, Wang B, Stockand JD (2014) Restrictive Expression of Acid-Sensing Ion Channel 5 (Asic5) in Unipolar Brush Cells of the Vestibulocerebellum. PLoS ONE 9(3): e91326. doi:10.1371/journal.pone.0091326

**Editor:** Candice Askwith, The Ohio State University, United States of America

**Received:** November 4, 2013; **Accepted:** February 7, 2014; **Published:** March 24, 2014

**Copyright:** © 2014 Boiko et al. This is an open-access article distributed under the terms of the Creative Commons Attribution License, which permits unrestricted use, distribution, and reproduction in any medium, provided the original author and source are credited.

**Funding:** This research was supported by the American Heart Association grant EIA 0640054N to JDS. The Core Optical Imaging Facility at UTHSCSA is supported by UTHSCSA and the NIH (NCI P30 CA54174 to the San Antonio Cancer Institute; NIA P30 AG013319 to the Nathan Shock Center; and NIA P01AG19316). The funders had no role in study design, data collection and analysis, decision to publish, or preparation of the manuscript.

**Competing Interests:** The authors have declared that no competing interests exist.

\* E-mail: stockand@uthscsa.edu

† These authors contributed equally to this work.

## Introduction

Degenerin/Epithelial Na<sup>+</sup> channel (Deg/ENaC) proteins comprise an ancient ion channel family that is expressed in every metazoan species [1]. Mammals express two general types of Deg/ENaC channels: acid-sensing ion channels (Asic) and ENaC [2–5]. ENaC is chiefly expressed in epithelial cells and is involved in Na<sup>+</sup> transport. Asics are expressed in neurons of the peripheral and central nervous systems. Asics are ligand-gated channels that conduct depolarizing inward Na<sup>+</sup> currents. This allows certain Asics, as typified by *Asic1* in hippocampal CA1 neurons, to function as post synaptic ionotropic receptors important to synaptic transmission [6]. Because they are sensitive to acid, Asic proteins also contribute to excitotoxic neuronal damage during ischemia and local acidosis [3,7,8]. Inappropriate Asic activity contributes to the progression and symptoms of several pathologies of the brain to include stroke and multiple sclerosis [8–11]. Consequently, these channels are an emerging target to treat such diseases. Sensitivity to acid also underlies involvement of Asics in pain sensing and them being targets for analgesics [8,12].

Mammals express five Asic genes: *Asic1-5*. While relatively much is understood about *Asic1-3* and to a lesser extent *Asic4*, *Asic5* is an orphan member of the family about which little is known. *Asic5* has been called the brain, liver, intestinal Na<sup>+</sup> channel (BLINaC), human intestinal Na<sup>+</sup> channel (hINaC), and bile acid-sensitive ion channel (BASIC) previously [13–15]. *Asic5*

mRNA is richly expressed in the brain and liver [13,14]. In the brain, *Asic5* mRNA is most abundant in the cerebellum and sparse in other areas [13]. In the liver, *Asic5* is expressed in the luminal membrane of epithelial cholangiocytes that line the bile duct and is activated by bile acid [15,16]. This is consistent with *Asic5* serving a Na<sup>+</sup> transport function akin to that of ENaC. The function of *Asic5* in the brain remains obscure. Moreover, it is unknown if *Asic5* is expressed in neurons or other brain cell types.

The goal of this study was to identify the specific region and type of cell in the brain that expresses *Asic5* to begin understanding the function of this orphan Deg/ENaC channel in the nervous system. Findings from a novel *Asic5* reporter mouse combined with single cell RT-PCR and electrophysiology demonstrate that *Asic5* is restrictively expressed in interneurons in the granular layer of the cerebellum, specifically in unipolar brush cells (UBC) of the vestibulocerebellum.

## Materials and Methods

### Materials

All chemicals and materials were purchased from Sigma unless noted otherwise. The Tg(Grp-EGFP)DV197Gsat mouse used in these studies was generated by the GENSAT project [17–19] and was obtained with permission from Drs. M. Martina and E. Mugnaini (Northwestern University, Evanston IL). In this

transgenic animal, GFP is primarily expressed in a subset of vestibulocerebellar UBCs that also express mGluR1 $\alpha$ .

### Animal use and care

All animal use and welfare adhered to the National Institutes of Health Guide for the Care and Use of Laboratory Animals following a protocol reviewed and approved by the Institutional Animal Care and Use Committee of the University of Texas Health Science Center at San Antonio. Experimental mice were housed and cared for by Laboratory Animal Resources at the University of Texas Health Science Center at San Antonio, which is fully accredited by the Association for Assessment and Accreditation of Laboratory Animal Care, and licensed by the United States Department of Agriculture.

### Generation and genotyping of the *Asic5* reporter mouse

The *Asic5<sup>tm2a(KOMP)Wtsi</sup>* targeting vector (ID: 33140) was purchased from the Knockout Mouse Project (KOMP) Repository at the University of California Davis and Children's Hospital Oakland Research Institute. This targeting vector contains the SA- $\beta$ geo-pA gene trapping cassette and produces a knockout first allele that is reporter-tagged and has conditional potential. This targeting vector contains a splice acceptor (En2 SA) and a polyadenylation tract (pA) upstream and downstream, respectively, of *lacZ*, and has a downstream *neo* gene driven by a separate promoter. Exon2 and 3 encode nucleotides 41–348 and 349–587 of the *Asic5* coding sequence (Transcript ID: ENSMUST0000029641). The intron between exon2 and 3 is 4555 nucleotides long. The SA- $\beta$ geo-pA trapping cassette replaces one hundred nucleotides of this intronic sequence in the *Asic5<sup>tm2a(KOMP)Wtsi</sup>* targeting vector.

Congenic germline transmitting chimeras were generated for the Stockand laboratory by the Mouse Biology Program at the University of California Davis through a fee for service agreement. In brief, the *Asic5<sup>tm2a(KOMP)Wtsi</sup>* targeting vector was electroporated into JM8A3.N1 (Agouti) embryonic stem cells [20]. A suitable clone positive for homologous recombination was then injected into blastocysts from a B6D2F1 $\times$ C57BL/6 donor.

Mouse genomic DNA was extracted from tail samples using the DNeasy Blood and Tissue Kit (Qiagen) following the manufacturer's instructions. For genotyping, a standard polymerase chain reaction was performed with this genomic DNA using the MangoMix PCR Kit (Bioline). The allele specific primers used in these reactions were: 1. forward common 5'-AGCT-GACTGCTGGCTGGTTATGTG-3'; 2. reverse wild type 5'-TTTGCTTAACTGACCATAAAGGC-3'; and 3. reverse reporter 5'-TCCTCTACATAGTTGGCAGTGTTC-3'.

Long range PCR was used to confirm homologous recombination and to define the site of insertion. For long range PCR, genomic DNA was isolated as above and amplified using Phusion Hot Start II High-Fidelity DNA Polymerase (Fisher Scientific). The forward 5'-AGCCTCTGATTGCAGATGGACCTCA-3' primer, which is outside the homology arm, was used in combination with the reverse 5'-GGTGGTGTGGAAAGG-GTTTCGAAG-3' primer, which is unique to the targeting vector, to amplify across the 5' insertion site. Following homologous recombination, this primer set will produce a 5,342 bp product with no product amplified from the wild type allele. The forward 5'-AGCCTCTGATTGCAGATGGACCTCA-3' primer, which is unique to the targeting vector, was used in combination with the reverse 5'-GGTGGTGTGGAAAGG-GTTTCGAAG-3' primer, which is outside the homology arm, to amplify across the 3' insertion site. Following homologous recombination, this primer

set will produce a 5,110 bp product with no product amplified from the wild type allele.

### RT-PCR

RNA was isolated from the cerebellum and liver using the RNeasy Kit (Qiagen) according to the manufacturer's instructions. First strand cDNA was prepared using the ProtoScript First Strand cDNA Synthesis Kit (NE BioLabs). PCR was then performed using the iProof High Fidelity PCR Kit (Bio-Rad Laboratories). The primers used to identify *lacZ* and  $\beta$ -actin mRNA were: forward 5'-GATTACCGTTGATGTTGAAGTGG-3' and reverse 5'-GGGAAGACGTACGGGGTATACAT-3; and forward 5'-TTCCTTCTTGGGTATGGAATCCTG-3' and reverse 5'-GTGTAACACGCAGCTCAGTAACAGT-3', respectively.

### Single-cell RT-PCR

Single cell RT-PCR followed standard protocols. In brief, the vestibulocerebellums of Tg(Grp-EGFP)DV197Gsat mice were dissected away from meninges in ice-cold Hank's Balanced Salt Solution (HBSS), cut into small pieces and digested with 3 mg/ml protease XXIII at 31°C for 7 minutes [21–23]. Digestion was terminated with 1 mg/ml BSA and 1 mg/ml trypsin inhibitor. A dissociated cell suspension was created from this digestion by mechanical trituration. Dissociated neurons were plated on poly-D-lysine-coated glass coverslips in Tyrode's solution. GFP-positive UBCs were identified by morphology and GFP emissions. Individual GFP-positive UBCs and GFP-negative vestibulocerebellar neurons were captured in a glass micropipette filled with Tyrode's solution using gentle suction. RNA from individual cells was isolated and reverse transcribed using the SuperScript III CellsDirect cDNA Synthesis System (Life Technologies). PCR was then performed as above with the iProof High Fidelity PCR Kit (Bio-Rad Laboratories). Primers used to detect *Asic5* and actin mRNA in these reactions were: forward 5'-AGTCGTTTGGT-CAATTACTTCACAT-3' and reverse 5'-AAAAAC-CATTGTTCTTGACAAACTC-3'; and forward 5'-TTCCTTCTTGGGTATGGAATCCTG-3' and reverse 5'-GTGTAACACGCAGCTCAGTAACAGT-3', respectively.

### Staining for $\beta$ -galactosidase activity

Deeply anesthetized mice were perfused transcardially with saline and then ice cold 2% paraformaldehyde in PBS. Sagittal and coronal (200  $\mu$ m) sections were prepared using a vibratome from the brains or cerebellums of these mice. Sections were stained with  $\beta$ -Gal substrate following a standard protocol [24]. In brief, sections were post-fixed with 0.2% glutaraldehyde, permeabilized with 0.2% Tween 20 and stained overnight at 37°C with 1 mg/ml X-Gal in PBS supplemented with 5 mM K<sub>3</sub>[Fe(CN)<sub>6</sub>], 5 mM K<sub>4</sub>[Fe(CN)<sub>6</sub>], 2 mM MgCl<sub>2</sub> and 0.2% Tween 20. Images of  $\beta$ -galactosidase activity in cerebellar sections were acquired using a MZ16 stereomicroscope (Leica).

### Immunohistochemistry

Perfusion fixed murine brains were harvested as above and subsequently fixed an additional two hours at 4°C with 2% paraformaldehyde. Brains were then cryoprotected with 20% glucose at 4°C for 24–48 hours. Sagittal cryosections (14  $\mu$ m) through the vermis of dissected cerebellums were prepared on a freezing-stage microtome and subsequently mounted on charged superfrost-plus glass slides. Sections were blocked for 30 minutes at room temperature with 3% BSA in PBS containing 0.1% Triton X-100 and then incubated with primary antibody at 4°C overnight. Sections then were exposed to appropriate secondary

antibodies as normal. Secondary antibodies were conjugated to Alexa 488 or Alexa 568 (Life Technologies). Fluorescence images of cerebellar sections and UBCs were acquired using an IX81/FV-1000 confocal microscope (Olympus) housed within the Core Optical Imaging Facility at UTHSCSA. The following primary antibodies were used in the current studies: rabbit anti- $\beta$ -galactosidase (1:5,000; MP Biomedicals), mouse anti-mGluR1 $\alpha$  (1:200; BD Biosciences), mouse anti-calretinin (1:1000; Millipore), and mouse anti-GFP (1:5000; Millipore). Cerebellum sections probed with mouse primary antibodies were treated with M.O.M IgG blocking reagent (Vector Laboratories) to minimize nonspecific cross reactivity.

### Electrophysiology in cerebellar slices

Brain slices were prepared from 3–4 week old mice following proven protocols used previously to record from vestibulocerebellar granular layer interneurons to include UBCs [25,26]. In brief, freshly harvested cerebellums were placed in ice-cold cutting solution containing (in mM): 87 NaCl, 25 NaHCO<sub>3</sub>, 2.5 KCl, 1.25 NaH<sub>2</sub>PO<sub>4</sub>, 0.5 CaCl<sub>2</sub>, 7 MgCl<sub>2</sub>, 75 sucrose, 25 glucose, 0.4 vitamin C and 1 kynurenic acid, bubbled with 95% O<sub>2</sub>-5% CO<sub>2</sub>. Parasagittal slices (300  $\mu$ m) were prepared using a vibratome. Slices then were maintained in a physiological extracellular solution containing (in mM) 125 NaCl, 25 NaHCO<sub>3</sub>, 1.25 NaH<sub>2</sub>PO<sub>4</sub>, 2.5 KCl, 1.2 CaCl<sub>2</sub>, 1 MgCl<sub>2</sub>, 25 glucose and 0.4 vitamin C (bubbled with 95% O<sub>2</sub>-5% CO<sub>2</sub>) at 30°C for 1 hour and then moved to room temperature.

For patch-clamping, interneurons in the granular layer of lobules IX and X were visualized with infrared/DIC videomicroscopy using a 60 $\times$  water-immersion objective on an upright BX51WI microscope (Olympus). GFP-expressing UBCs were identified with epifluorescence illumination. Patch electrodes (5–9 M $\Omega$ ) were fabricated from borosilicate glass capillaries (B150-86-10, Sutter Instrument) using a horizontal puller. The intracellular recording solution contained (in mM): 140 K-gluconate, 2 MgCl<sub>2</sub>, 10 EGTA, 2 Na<sub>2</sub>ATP, 0.1 NaGTP and 10 Hepes, pH 7.3. Whole-cell current-clamp recordings were performed using a HEKA EPC10 amplifier and the Patchmaster software (HEKA Instruments). Data were sampled at 40  $\mu$ s intervals and low-pass filtered at 7.2 kHz using a four-pole Bessel filter. Neurons were held at –70 mV. Input resistance was estimated using a –20 pA current injection. Action potentials were elicited by supra-threshold current injections of 1 second.

### Data Analysis and Comparison

Contrast maps of  $\beta$ -galactosidase activity were generated using paint.net with the Selective Enhancer plug-in. Plug-in parameters were set to maximize contrast. Transverse renderings are maximal intensity projections of the 3D-stacks. Sections in these transverse renderings were aligned according to the Allen Brain Atlas ([www.brain-map.org](http://www.brain-map.org)).

Analysis of action potentials was performed using the Axo-GraphX software (Kagi). For evaluation of individual action potential properties, the 1<sup>st</sup> and 2<sup>nd</sup> action potential waveforms elicited by a 30-pA current injection were used. Data were statistically analyzed using KaleidaGraph (Synergy Software) and graphed using Igor Pro (WaveMetrics).

All summarized data reported as mean  $\pm$  SEM. Unpaired data and proportions were compared with a *t*-test and *Z*-test, respectively. The criterion for significance was  $P \leq 0.05$ .

## Results

### The *Asic5*<sup>tm2a(KOMP)Wtsi</sup> mouse

The simplified scheme shown in figure 1A depicts the wild type *Asic5* and *Asic5*<sup>tm2a(KOMP)Wtsi</sup> alleles. Also shown are the relative binding sites and orientation of genotyping primers. The forward common primer 1 interacts with a sequence within intron 2–3 that is in both the wild type and reporter allele. The reverse wild type primer 2 interacts with an intronic sequence in the wild type allele not found in the reporter allele. The reverse reporter primer 3 interacts with sequence unique to the gene trapping cassette and thus is only in the *Asic5*<sup>tm2a(KOMP)Wtsi</sup> allele. Figure 1B shows typical results from genotyping experiments on mice homozygous for the wild type or reporter allele using these primers. As expected the combination of primers 1 and 2 produced a PCR product of predicted size from wild type mice that was absent in *Asic5*<sup>tm2a(KOMP)Wtsi</sup> mice. Primers 1 and 3 produced a product of predicted size from reporter mice that was absent in wild type littermates.

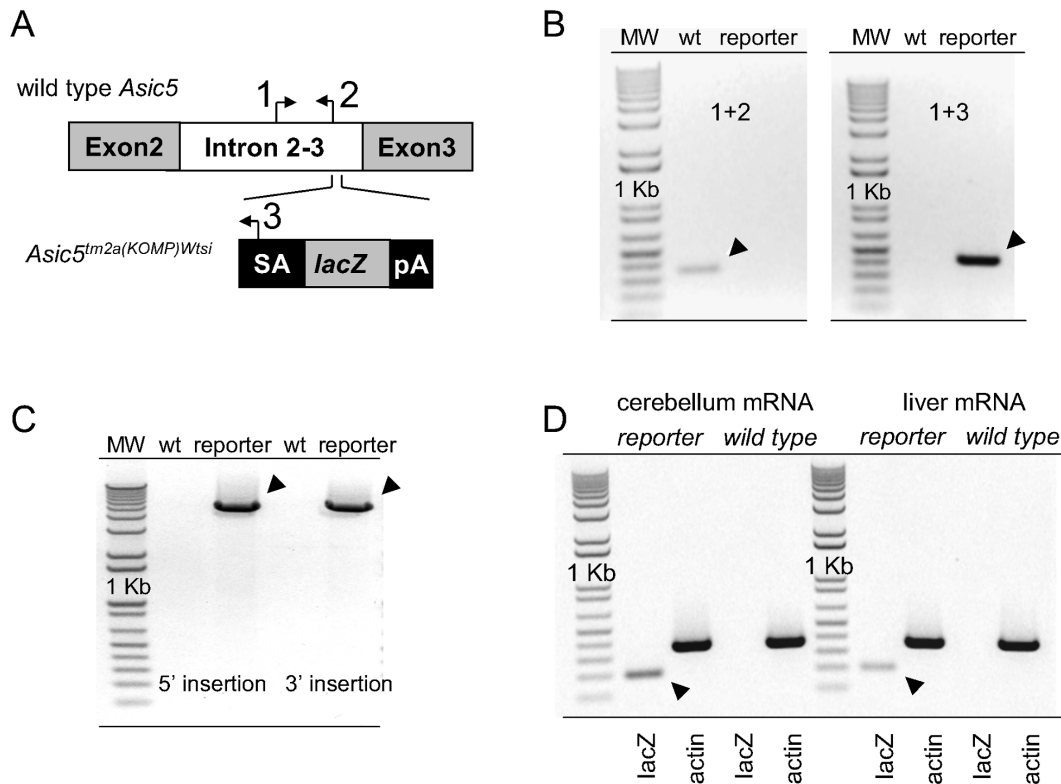
To confirm proper genomic targeting, the site of insertion of the targeting vector was mapped with long range PCR across both insertion arms. As shown in figure 1C insertion was at the expected site.

Figure 1D shows typical results from RT-PCR experiments probing expression of lacZ mRNA in the cerebellum and liver of homozygous *Asic5*<sup>tm2a(KOMP)Wtsi</sup> mice and wild type littermates. *Asic5* mRNA has previously been shown to be expressed in these tissues [13,14]. As expected, lacZ mRNA was expressed in the cerebellums and livers of *Asic5*<sup>tm2a(KOMP)Wtsi</sup> mice but not wild type littermates.

### *Asic5* is restrictively expressed in interneurons in the granular layer of the vestibulocerebellum

Figure 2A shows typical staining for  $\beta$ -galactosidase activity in three representative coronal slices of the cerebellum from the *Asic5*<sup>tm2a(KOMP)Wtsi</sup> mouse. Figure 2B shows a contrast map of  $\beta$ -galactosidase staining in sequential sections through the entire cerebellum (and a portion of the brainstem). Raw data were from experiments identical to that in 2A. Also shown in 2B is a composite contrast rendering of the whole cerebellum (and part of the brainstem) viewed from the transverse plane. In the reporter animal, staining of  $\beta$ -galactosidase activity in the cerebellum was strong and chiefly restricted to the ventrocaudal region of the vermis in the posterior and flocculonodular lobes corresponding to the vestibulocerebellum; and in the brainstem in the dorsal cochlear nucleus. Little staining was observed in the brain of the reporter mouse outside of the cerebellum and no staining was seen in the cerebellum of wild type littermates. Staining outside of the cerebellum in the brain of the reporter mouse, as shown in figure S1, was sparse and punctuate in nature being localized to a small region of the cortex and the olfactory tubercle.

Shown in figure 3A with an enlargement of the area containing the vestibulocerebellum reproduced in 3B is a representative midsagittal section of the cerebellum of the *Asic5*<sup>tm2a(KOMP)Wtsi</sup> mouse stained for  $\beta$ -galactosidase activity. As above for coronal sections, figure 3C shows a contrast map of  $\beta$ -galactosidase staining in sagittal sections through half of the cerebellum and a composite contrast rendering of staining in the whole cerebellum viewed from the transverse plane.  $\beta$ -galactosidase activity was restricted to interneurons in the granular layer of the vestibulocerebellum chiefly in lobules X and IXb and IXc, but notably not IXa. These regions of the mouse cerebellum correspond to the ventral uvula and nodulus in the human.



**Figure 1. The *Asic5<sup>tm2a(KOMP)Wtsi</sup>* mouse.** A. A simplified scheme showing the wild type *Asic5* (top) and reporter *Asic5<sup>tm2a(KOMP)Wtsi</sup>* (bottom) alleles as well as the orientation and relative positions of binding sites for primers used in genotyping reactions. The *neo* gene in the trapping cassette is not shown in this figure. B. Inverted images of representative gels ( $n \geq 60$ ) containing typical products from genotyping reactions of homozygous wild type and *Asic5<sup>tm2a(KOMP)Wtsi</sup>* reporter mice using primers 1, 2 & 3. Expected products are indicated with arrowheads. C. Inverted image of a representative gel ( $n > 3$ ) containing the products of long range PCR reactions across both insertion arms. D. Inverted images of representative gels containing typical RT-PCR products generated from mRNA isolated from the cerebellum (left) and liver (right) of *Asic5<sup>tm2a(KOMP)Wtsi</sup>* mice and wild type littermates. Primers specific for *lacZ* and *actin* mRNAs were used in these reactions with *actin* serving as a positive control. Arrowheads indicate the expected *lacZ* product.

doi:10.1371/journal.pone.0091326.g001

### *Asic5* is expressed in unipolar brush cells

UBCs are excitatory glutamatergic interneurons common to the granular layer of the vestibulocerebellum, lobules X and IXb-c but not IXa, that are sparse throughout the rest of the cerebellum and brain [27–30]. UBCs have a characteristic morphology. As shown in figure 4 and figures S2, S3, S4,  $\beta$ -Gal expressing cerebellar interneurons in the *Asic5<sup>tm2a(KOMP)Wtsi</sup>* mouse had a distinctive morphology including a short but broad dendrite that terminated in an extended dendriole. Such morphology is a hallmark of UBCs and was common to every  $\beta$ -Gal positive cell observed in the reporter mouse in these studies [27–30].

Strong expression of the metabotropic glutamate receptor 1 $\alpha$  (mGluR1 $\alpha$ ) is also a hallmark of a majority of UBCs. Consequently, anti-mGluR1 $\alpha$  staining has been used previously to demonstrate expression of this type of interneuron in the granular layer of lobules X and IXb-c [19,31,32]. As shown in figure S2, interneurons labeled with anti-mGluR1 $\alpha$  antibody in the wild type mouse have an expression pattern similar to that of those positive for  $\beta$ -Gal in the *Asic5<sup>tm2a(KOMP)Wtsi</sup>* mouse. Both are enriched in the granular layers of lobules X and IXb and IXc, but not IXa. (The modest labeling of Purkinje cells by anti- $\beta$ -Gal antibody shown in figure S2 is nonspecific as it was also observed in the cerebellum of wild type animals, as shown in figure S3, and as compared to labeling of UBCs which was specific to the reporter animal and not observed in wild type littermates.)

To further establish the identity of *Asic5* expressing cells, sagittal sections of the cerebellum of the *Asic5<sup>tm2a(KOMP)Wtsi</sup>* reporter mouse were co-labeled with anti-mGluR1 $\alpha$  and anti- $\beta$ -Gal antibodies. As shown in figure 4 and figure S4, anti-mGluR1 $\alpha$  and  $\beta$ -Gal antibodies labeled the same interneuron with the prior antibody primarily labeling dendriole brushes as expected.

### *Asic5* is expressed chiefly in mGluR1 $\alpha$ (+) UBCs

There are at least two major subtypes of UBCs. Those that richly express mGluR1 $\alpha$  termed mGluR1 $\alpha$  (+) and those that express calretinin termed CR (+) [19,32]. The prior represents the majority, approximately 2/3, of the UBCs in the vestibulocerebellum and the latter about 1/3. Interestingly, mGluR1 $\alpha$  (+) but not CR (+) UBCs are expressed throughout lobules X and IXb-c [19]. In comparison, CR (+) UBCs are expressed only in lobule X and the anterior portion of lobule IXc. Thus, the expression pattern of mGluR1 $\alpha$  (+) UBCs best corresponds with those expressing *Asic5* as assessed in the reporter mouse. To further explore this possibility, we co-labeled sagittal sections from the reporter mouse with anti-calretinin and anti- $\beta$ -Gal antibodies. As is clear in the representative fluorescence micrograph shown in figure S5, anti-CR and anti- $\beta$ -Gal antibodies label distinct populations of UBCs. Indeed, no cell was found to be co-stained by both antibodies in these experiments.

As shown previously, GFP expression in the Tg(Grp-EGFP)DV197Gsat mouse is chiefly in mGluR1 $\alpha$  (+) UBCs

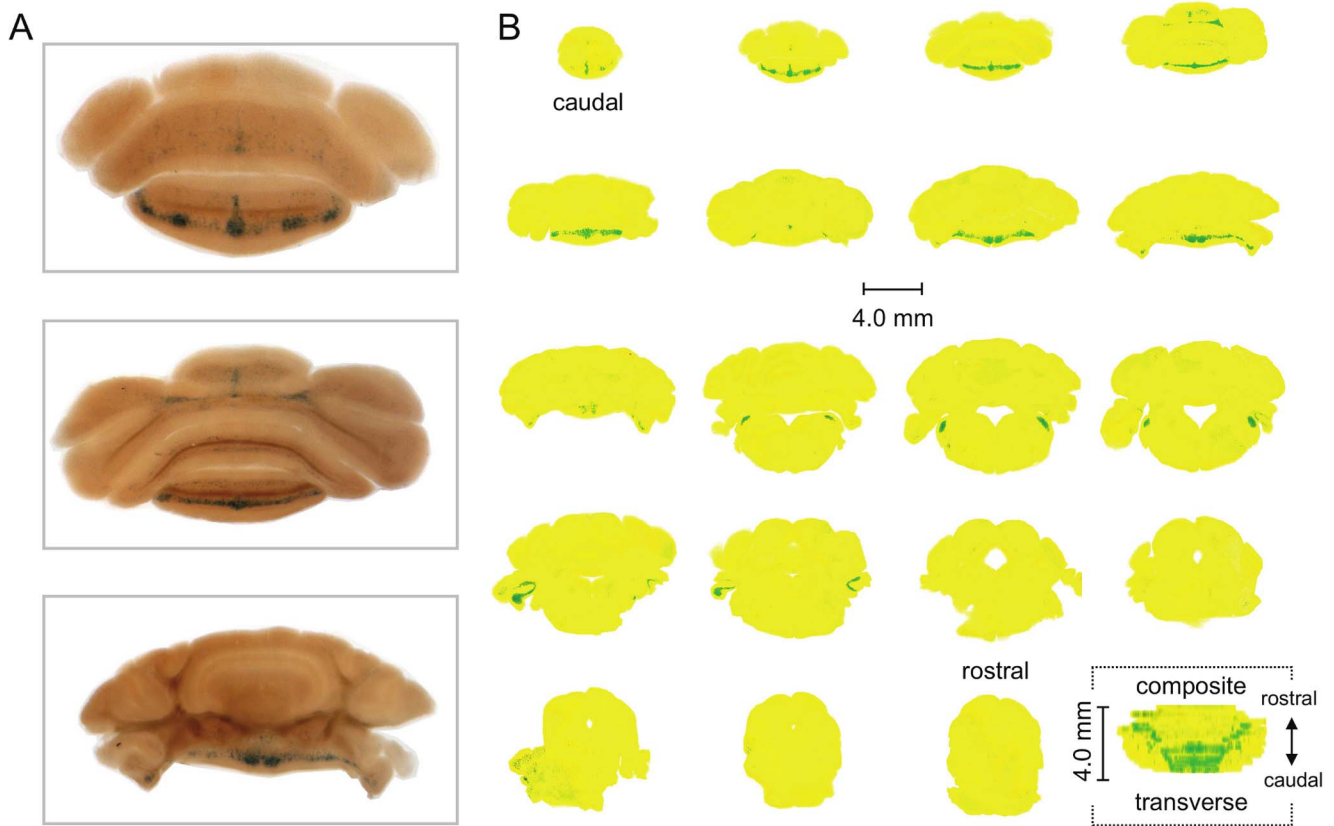


**Figure 2.  $\beta$ -Gal is restrictively expressed in the vestibulocerebellum of the  $Asic5^{tm2a(KOMP)Wtsi}$  mouse.** A. Representative images of coronal sections (200  $\mu$ m) through the cerebellum and brainstem of the reporter mouse stained for  $\beta$ -galactosidase activity (blue). Slices are displayed in a caudal to rostral arrangement with the top being the most caudal of the three. The top, middle and bottom slices correspond with the 2<sup>nd</sup>, 4<sup>th</sup> and 8<sup>th</sup> sections shown in 2B. B. Nineteen sequential coronal sections through the entire cerebellum (and part of the brainstem) of the  $Asic5^{tm2a(KOMP)Wtsi}$  mouse. Sections are shown in a caudal to rostral arrangement with the top left being the most caudal and the lower right (second to last) being the most rostral. Raw data are identical to that shown in 2A. Images were color and contrast manipulated to emphasize staining for  $\beta$ -galactosidase activity with yellow representing no staining and green representing robust staining. The final image in 2B represents a composite of the whole cerebellum (and part of the brainstem) collapsed into a 2-D rendering shown in the transverse plane. This rendering is a compilation of the 19 coronal sections shown in 2B stacked caudal to rostral, flipped 90° and collapsed. doi:10.1371/journal.pone.0091326.g002

[18,19]. The current study took advantage of this. Figure 5 shows a representative midsagittal section through the vermis of the cerebellum stained with anti-GFP and anti- $\beta$ -Gal antibodies from a mouse homozygous for the  $Asic5^{tm2a(KOMP)Wtsi}$  reporter allele and that also had at least one copy of the Tg(Grp-EGFP) transgene. Similar to mGluR1 $\alpha$  as shown above, GFP expression in these animals strongly overlapped with that of  $Asic5$ , as assessed by expression of  $\beta$ -Gal, with significant co-localization in interneurons in the granular layer of lobules X and IXb-c.

Single-cell RT-PCR findings from the Tg(Grp-EGFP)DV197Gsat mouse further support that a significant portion of mGluR1 $\alpha$  (+) UBCs express  $Asic5$ . A representative observation and corresponding summary graph of such experiments are shown in figure 6. A significant proportion of GFP-positive UBCs in the Tg(Grp-EGFP)DV197Gsat mouse expressed  $Asic5$  mRNA. In contrast,  $Asic5$  mRNA was never observed in cerebellar neurons that lacked GFP in the transgenic animal.

#### UBCs enriched in $Asic5$ have electrical properties consistent with those positive for mGluR1 $\alpha$

The electrophysiological properties of granular cells (GC) and GFP-positive UBCs in the transgenic animal, which as shown above are enriched in  $Asic5$ , were determined next in vestibulo-

cerebellar slices. As shown by the typical traces from representative current clamped GCs and GFP-positive UBCs, and corresponding summary graphs of resting membrane potential, input resistance and capacitance in figure S6, GCs and GFP-positive UBCs were distinguishable by their respective electrical properties. As compared to GCs, the input resistance and capacitance of GFP-positive UBCs in the Tg(Grp-EGFP)DV197Gsat mouse were lesser and greater in magnitude, respectively. The resting membrane potential of GFP-positive UBCs was also more depolarized compared to GCs. These findings are consistent with similar electrophysiological results published previously showing that the majority of GFP-positive interneurons in the the Tg(Grp-EGFP)DV197Gsat mouse are mGluR1 $\alpha$  (+) UBCs [19,25,33].

As compared to GCs and CR (+) UBCs which intrinsically and regularly fire action potentials, mGluR1 $\alpha$  (+) UBCs fire little at rest and show a bursting phenotype when stimulated [19,25,33]. This was reaffirmed in the present study as shown in figure S7. This provides further evidence that the population of UBCs enriched in  $Asic5$ , as followed by GFP expression in the transgenic animal, are those that express mGluR1 $\alpha$ . Current clamped GCs and GFP-positive UBCs in vestibulocerebellar slices showed hallmark continuous and bursting firing patterns, respectively, in response to injection of a depolarizing supra-threshold current. In addition



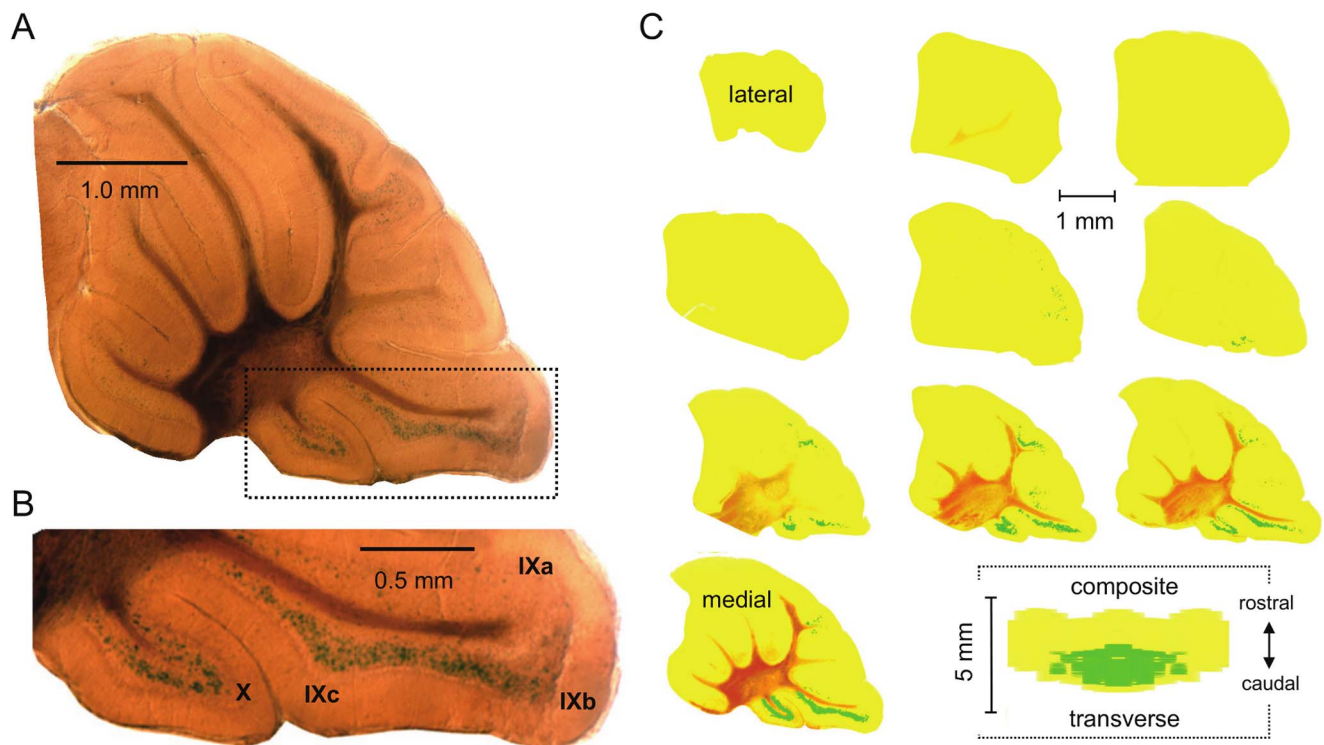


**Figure 3. *Asic5* is restrictively expressed in interneurons in the granular layer.** A. Representative midsagittal section (200  $\mu$ m) of the cerebellum from an *Asic5<sup>tm2a(KOMP)Wtsi</sup>* mouse stained for  $\beta$ -galactosidase activity. B. Lobules IX and X in the (boxed) section in 3A shown at a magnified scale. C. Ten sequential sagittal sections through one half of the entire cerebellum of the reporter mouse. Sections are shown in a lateral to medial arrangement with the top left being the most lateral and the lower right (second to last) closest to the midline. Raw data are identical to that shown in 3A. Images were color and contrast manipulated to emphasize staining for  $\beta$ -galactosidase activity with yellow representing no staining and green representing robust staining. The final image in 3C represents a composite of the whole cerebellum collapsed into a 2-D rendering shown in the transverse plane. This rendering is a compilation of the 10 sagittal sections shown in 3B stacked lateral to medial, flipped 90° and collapsed with the left half of this figure being a mirror image of the right.  
doi:10.1371/journal.pone.0091326.g003

to differences in characteristic firing patterns, the first and second action potentials in evoked trains of action potentials from GCs and GFP-positive UBCs had distinct properties. Action potentials in GFP-positive UBCs as compared to GCs had shorter inter-event intervals, were broader and had markedly smaller fast after hyperpolarizing potentials. In addition, whereas the 1<sup>st</sup> action potential in GFP-positive UBCs reached a significantly greater peak voltage compared to that in GCs, the next action potential peaked at a significantly lower voltage compared to the corresponding action potential in GCs.

## Discussion

The current findings demonstrate that *Asic5* is restrictively expressed in the brain in a subset of specialized interneurons that are localized to the granular layer of the vestibulocerebellum. The cerebellar interneurons which express *Asic5* are UBCs with this channel chiefly expressed in UBCs that also express mGluR1 $\alpha$ . This restrictive expression pattern has important implications for the cellular and physiological functions of this channel.

The current study makes several observations in support of *Asic5* being expressed in a restrictive manner in mGluR1 $\alpha$  (+) UBCs of the vestibulocerebellum. The *Asic5* reporter mouse shows little expression in the brain outside of the cerebellum but rich expression in this region. This expression profile agrees with that reported for *Asic5* in the Allen Mouse Brain Atlas (Website: 2012 Allen Institute for Brain Science. Allen Mouse Brain Atlas

[Internet]. Available from: <http://mouse.brain-map.org/>) [34]. Though, it is easily missed in the latter resource because of the restrictive and punctuate nature of *Asic5* expression in the brain and because the transcript for this channel, similar to that for most other ion channels, likely has a low copy number. In the cerebellum, expression is localized to the vestibulocerebellum. In the vestibulocerebellum expression is in interneurons in the granular layer of lobules X and IXb and IXc but not IXa. This is the region of the cerebellum where UBCs are found [19,28,31]. UBCs are sparse in other cerebellar folia. Like mGluR1 $\alpha$  (+) UBCs [19],  $\beta$ -Gal positive interneurons in the *Asic5<sup>tm2a(KOMP)Wtsi</sup>* reporter mouse are also richly expressed in lobules X and IXc and throughout IXb. In comparison, CR (+) UBCs are enriched in lobule X and the anterior portion of IXc but sparse in the posterior portion of IXc and the entirety of IXb [19,31].

The cellular morphology of  $\beta$ -Gal expressing cells in the granular layer of the vestibulocerebellum of the *Asic5<sup>tm2a(KOMP)Wtsi</sup>* reporter mouse is also consistent with them being UBCs. They have the hallmark single short but broad dendrite of UBCs that terminates in the characteristic expansive dendriole brush [27,29,30,35].

The immunohistochemical properties of  $\beta$ -Gal expressing interneurons in the reporter mouse in addition also are consistent with them being mGluR1 $\alpha$  (+) UBCs. A significant proportion of the  $\beta$ -Gal expressing interneurons in the reporter mouse also express mGluR1 $\alpha$ . In contrast, no  $\beta$ -Gal positive cell was positive for CR. Moreover, there is notable overlap between the

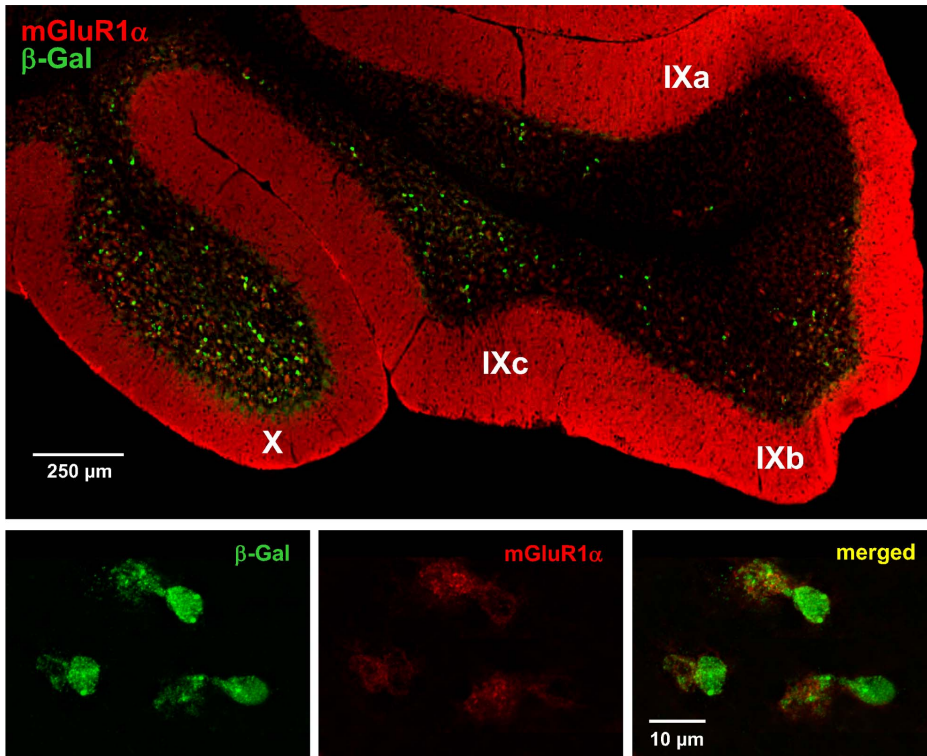


**Figure 4. *Asic5* is expressed in mGluR1 $\alpha$  (+) UBCs.** A representative fluorescence micrograph showing lobules IX and X in a typical midsagittal section of the cerebellum from the *Asic5<sup>tm2a(KOMP)Wtsi</sup>* mouse stained with anti- $\beta$ -Gal (green) and anti-mGluR1 $\alpha$  (red) antibodies. (This experiment was repeated with similar results in more than five different mice.) A region of lobule X that contains representative UBCs positive for both  $\beta$ -Gal (green; left) and mGluR1 $\alpha$  (red; middle) is shown at a magnified scale below with a merged image shown to the right.  
doi:10.1371/journal.pone.0091326.g004

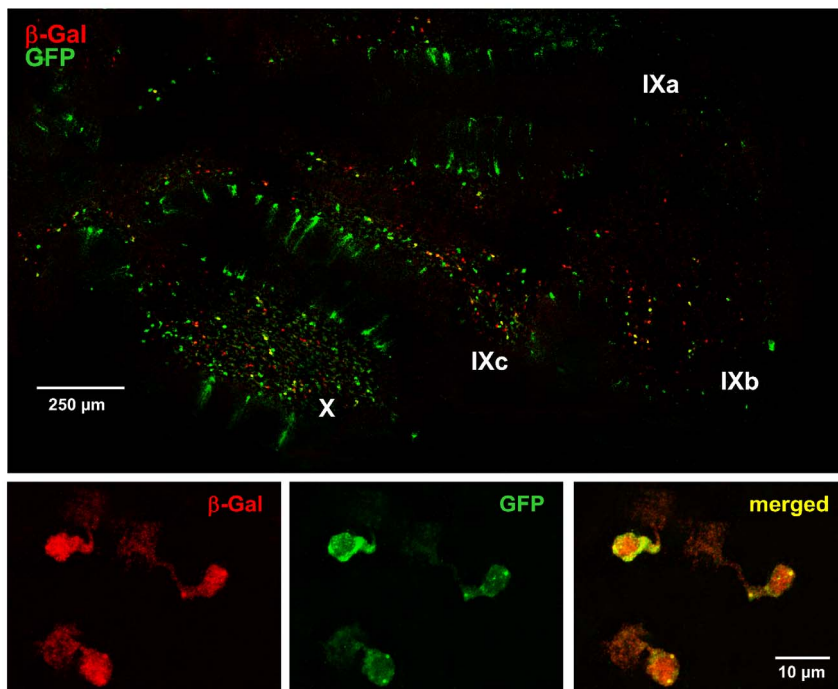


**Figure 5. *Asic5* is expressed in GFP-positive vestibulocerebellar interneurons in the Tg(Grp-EGFP)DV197Gsat mouse.** A representative fluorescence micrograph of a typical midsagittal section through the vermis of the cerebellum of a mouse that contains at least one copy of the Tg(Grp-EGFP) transgene and that is also homozygous for the *Asic5<sup>tm2a(KOMP)Wtsi</sup>* reporter allele. (This experiment was repeated with similar results in more than four different mice.) This section was probed with anti- $\beta$ -Gal (red) and anti-GFP (green) antibodies. A region of lobule IX that contains typical UBCs positive for both  $\beta$ -Gal (red; left) and GFP (green; middle) is shown at a magnified scale below. The merged image is shown to the right.  
doi:10.1371/journal.pone.0091326.g005

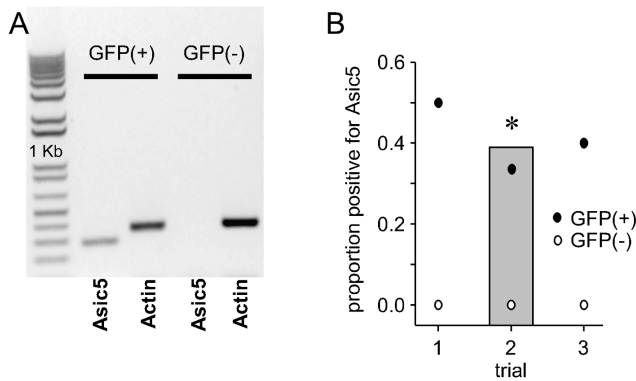


**Figure 6. Asic5 mRNA is restrictively expressed in mGluR1 $\alpha$  (+) UBCs.** A. Inverted image of a representative gel containing typical single-cell RT-PCR products from representative GFP-positive and GFP-negative vestibulocerebellar neurons from the Tg(Grp-EGFP)DV197Gsat mouse. Each cell was probed for expression of Asic5 mRNA with actin serving as an internal reaction control. B. Graph showing the proportion of GFP-positive and GFP-negative cells that expressed Asic5 mRNA in single-cell RT-PCR experiments using neurons from the vestibulocerebellum of three different Tg(Grp-EGFP)DV197Gsat mice. In this figure, open and closed circles show the proportion of GFP-negative and positive cells, respectively, that also expressed Asic5 mRNA in these three trials. In each of these trials more than four interneurons were tested per animal. The gray bar in this figure shows the total proportion of GFP-positive vestibulocerebellar interneurons from the Tg(Grp-EGFP)DV197Gsat mouse that also expressed Asic5. \*Significantly larger proportion as compared to GFP-negative cells. doi:10.1371/journal.pone.0091326.g006

population of interneurons that express  $\beta$ -Gal in the granular layer of the vestibulocerebellum in the reporter mouse and those that express GFP when the Tg(Grp-EGFP) transgene is introduced into this animal. GFP-positive cells in the Tg(Grp-EGFP)DV197Gsat mouse are recognized to be primarily mGluR1 $\alpha$  (+) UBCs [19].

Independent evidence consistent with Asic5 being restrictively expressed in mGluR1 $\alpha$  (+) UBCs comes from the observation that a significant portion of the GFP-positive but none of the GFP-negative cerebellar neurons tested in the Tg(Grp-EGFP)DV197Gsat mouse expressed Asic5 mRNA.

The final piece of evidence in these studies consistent with Asic5 being enriched in mGluR1 $\alpha$  (+) UBCs is that the GFP-positive cells, many of which also express  $\beta$ -Gal, in the Asic5 reporter/Tg(Grp-EGFP) transgenic mouse had electrical properties consistent with that reported previously for mGluR1 $\alpha$  (+) UBCs [19,25,26,29].

Considering its restrictive expression in the brain in mGluR1 $\alpha$  (+) UBCs, an important question is what is the function of Asic5 in these interneurons, and why do these cells in particular express this channel when other similar types of interneurons, for instance CR (+) UBCs in the vestibulocerebellum and granular cells in the wider cerebellum, do not appear to express this channel? Of the mammalian Asic and ENaC proteins, Asic5 is the most closely related to ancestral Deg/ENaC progenitors, including the neuropeptide-gated FaNaC and HyNaC channels expressed in mollusks and hydra, respectively [5,13,14]. Indeed, Asic5 shares approximately as much sequence identity with these primordial Deg/ENaC proteins as it does with other mammalian Asic proteins [13]. Ancestral Deg/ENaC proteins expressed in simpler animals in which nervous systems first developed, such as the hydra, function as post-synaptic ionotropic receptors for neuropeptides, as typified by RFamides, involved in fast synaptic transmission [1,36]. Perhaps Asic5 is an ortholog of these ancestral

channels that serves a similar function in mammals specifically in one of the oldest parts of the brain, the archicerebellum, which is another name for the vestibulocerebellum.

Irrespective of the specific function served by Asic5 in mGluR1 $\alpha$  (+) UBCs, the current findings are consistent with Asic5 being restrictively expressed in this subset of interneurons. This finding by its very nature argues that the function of Asic5 in these cells is critical and distinctive. Moreover, in consideration of the work previously done on Asic5 in liver epithelia [15,16], the current findings demonstrate that this channel performs at least two very distinct functions depending on whether it is expressed in neurons or epithelial cells. In neurons it most likely serves a function akin to that of other Asics and in epithelial cells one similar to ENaC.

## Supporting Information

**Figure S1**  $\beta$ -Gal expression outside of the cerebellum in the brain of the Asic5<sup>tm2a(KOMP)Wtsi</sup> mouse. Representative midsagittal section (200  $\mu$ m) through the brain of an Asic5<sup>tm2a(KOMP)Wtsi</sup> mouse stained for  $\beta$ -galactosidase activity. Areas of the cortex and olfactory tubercle are shown at a magnified scale. Dashed black lines show the relative positions of these magnified regions in the whole brain - Arrows note staining. The white asterisk notes staining in the vestibulocerebellum similar to that shown at higher magnification in figures 2 & 3.

(PDF)

**Figure S2** Asic5 is restrictively expressed in unipolar brush cells. Fluorescence micrographs showing lobules IX and X in typical midsagittal sections of the cerebellum from Asic5<sup>tm2a(KOMP)Wtsi</sup> (A) and Asic5 wild type (B) mice stained with anti- $\beta$ -Gal (green; A) and anti-mGluR1 $\alpha$  (red; B) antibodies, respectively. An area of lobule X from the reporter mouse that contains a representative  $\beta$ -Gal positive interneuron is shown at a magnified scale (boxed). The cell soma and hallmark dendriole brush for this UBC are noted. Modest labeling of Purkinje cells by the  $\beta$ -Gal antibody is nonspecific as it is also present in cerebellum from wild type animals (see figure S3).

(PDF)

**Figure S3** Non-specific staining of Purkinje cells by the anti- $\beta$ -Gal antibody. Representative fluorescence micrographs showing lobules IX and X in typical midsagittal sections of the cerebellum from Asic5 wild type mice stained with anti- $\beta$ -Gal (green) antibody.

(PDF)

**Figure S4** mGluR1 $\alpha$  (+) UBCs express  $\beta$ -Gal in the Asic5<sup>tm2a(KOMP)Wtsi</sup> mouse. A fluorescence micrograph showing a close-up view of a typical mGluR1 $\alpha$  (+) UBC in lobule X of the Asic5<sup>tm2a(KOMP)Wtsi</sup> reporter mouse that also expressed  $\beta$ -Gal. Anti-mGluR1 $\alpha$  and  $\beta$ -Gal staining are red and green, respectively. The cell soma and hallmark dendriole brush of this representative UBC are noted.

(PDF)

**Figure S5** CR (+) UBCs do not express  $\beta$ -Gal in the Asic5<sup>tm2a(KOMP)Wtsi</sup> mouse. A representative fluorescence micrograph showing lobules IX and X in a typical midsagittal section of the cerebellum from an Asic5<sup>tm2a(KOMP)Wtsi</sup> reporter mouse stained with anti-CR (red) and anti- $\beta$ -Gal (green) antibodies. Areas from lobule X containing CR (+) and  $\beta$ -Gal-positive UBCs are shown at a magnified scale (boxed). The cell soma and hallmark dendriole brushes of these representative types of UBCs are noted.

(PDF)

**Figure S6** Electrical properties of GFP-positive vestibulocerebellar interneurons in the Tg(Grp-EGFP)DV197Gsat mouse. A.



Representative traces from typical GCs (middle) and GFP-positive UBCs (bottom) in vestibulocerebellar slices from a wild type and Tg(Grp-EGFP)DV197Gsat mouse. These interneurons were current-clamped at rest and then subjected to a hyperpolarizing (−20 pA) current injection (waveform shown at top). Inset shows a clamped UBC that was back-filled with lucifer yellow to allow post-hoc analysis of morphology. The dendriole brush and soma of this UBC are noted. B. Summary graphs of the mean resting membrane potential (top), input resistance (middle) and capacitance (bottom) of GCs and GFP-positive UBCs in vestibulocerebellar slices. Data collected from experiments identical to that in S6A. Also shown in these graphs are the individual data points collected for each cell type. Individual GCs and UBCs were recorded from both wild type and Tg(Grp-EGFP)DV197Gsat mice with the bulk of the data points for the former coming from the wild type animal and the latter the transgenic animal. (PDF)

**Figure S7** GFP-positive vestibulocerebellar interneurons of the Tg(Grp-EGFP)DV197Gsat mouse have a distinctive bursting

## References

- Golubovic A, Kuhn A, Williamson M, Kalbacher H, Holstein TW, et al. (2007) A peptide-gated ion channel from the freshwater polyp Hydra. *J Biol Chem* 282: 35098–35103.
- Bianchi L, Driscoll M (2002) Protons at the gate: DEG/ENaC ion channels help us feel and remember. *Neuron* 34: 337–340.
- Sherwood TW, Frey EN, Askwith CC (2012) Structure and activity of the acid-sensing ion channels. *Am J Physiol Cell Physiol* 303: C699–C710.
- Garty H, Palmer LG (1997) Epithelial sodium channels: function, structure, and regulation. [Review] [451 refs]. *Physiological Reviews* 77: 359–396.
- Kellenberger S, Schild L (2002) Epithelial sodium channel/degnerin family of ion channels: a variety of functions for a shared structure. *Physiol Rev* 82: 735–767.
- Zha XM, Wemmie JA, Green SH, Welsh MJ (2006) Acid-sensing ion channel 1a is a postsynaptic proton receptor that affects the density of dendritic spines. *Proc Natl Acad Sci U S A* 103: 16536–16561.
- Chu XP, Xiong ZG (2013) Acid-sensing ion channels in pathological conditions. *Adv Exp Med Biol* 961: 419–431.
- Leng TD, Xiong ZG (2013) The pharmacology and therapeutic potential of small molecule inhibitors of acid-sensing ion channels in stroke intervention. *Acta Pharmacol Sin* 34: 33–38.
- Xiong ZG, Pignataro G, Li M, Chang SY, Simon RP (2008) Acid-sensing ion channels (ASICs) as pharmacological targets for neurodegenerative diseases. *Curr Opin Pharmacol* 8: 25–32.
- Friese MA, Craner MJ, Etzensperger R, Vergo S, Wemmie JA, et al. (2007) Acid-sensing ion channel-1 contributes to axonal degeneration in autoimmune inflammation of the central nervous system. *Nat Med* 13: 1483–1489.
- Vergo S, Craner MJ, Etzensperger R, Attfield K, Friese MA, et al. (2011) Acid-sensing ion channel 1 is involved in both axonal injury and demyelination in multiple sclerosis and its animal model. *Brain* 134: 571–584.
- Diochot S, Baron A, Salinas M, Douguet D, Scarzello S, et al. (2012) Black mamba venom peptides target acid-sensing ion channels to abolish pain. *Nature* 490: 552–555.
- Sakai H, Lingueglia E, Champigny G, Mattei MG, Lazdunski M (1999) Cloning and functional expression of a novel degnerin-like Na<sup>+</sup> channel gene in mammals. *J Physiol* 519 Pt 2: 323–333.
- Schaefer L, Sakai H, Mattei M, Lazdunski M, Lingueglia E (2000) Molecular cloning, functional expression and chromosomal localization of an amiloride-sensitive Na<sup>(+)</sup> channel from human small intestine. *FEBS Lett* 471: 205–210.
- Wiemuth D, Sahin H, Falkenburger BH, Lefevre CM, Wasmuth HE, et al. (2012) BASIC—a bile acid-sensitive ion channel highly expressed in bile ducts. *FASEB J* 26: 4122–4130.
- Wiemuth D, Sahin H, Lefevre CM, Wasmuth HE, Grunder S (2013) Strong activation of bile acid-sensitive ion channel (BASIC) by ursodeoxycholic acid. *Channels* 7: 38–42.
- Doyle JP, Dougherty JD, Heiman M, Schmidt EF, Stevens TR, et al. (2008) Application of a translational profiling approach for the comparative analysis of CNS cell types. *Cell* 135: 749–762.
- Gong S, Zheng C, Doughty ML, Losos K, Didkovsky N, et al. (2003) A gene expression atlas of the central nervous system based on bacterial artificial chromosomes. *Nature* 425: 917–925.
- Kim JA, Sekerkova G, Mugnaini E, Martina M (2012) Electrophysiological, morphological, and topological properties of two histochemically distinct subpopulations of cerebellar unipolar brush cells. *Cerebellum* 11: 1012–1025.
- Pettitt SJ, Liang Q, Rairdan XY, Moran JL, Prosser HM, et al. (2009) Agouti C57BL/6N embryonic stem cells for mouse genetic resources. *Nat Methods* 6: 493–495.
- Regan IJ (1991) Voltage-dependent calcium currents in Purkinje cells from rat cerebellar vermis. *J Neurosci* 11: 2259–2269.
- Raman IM, Bean BP (1997) Resurgent sodium current and action potential formation in dissociated cerebellar Purkinje neurons. *J Neurosci* 17: 4517–4526.
- Grieco TM, Afshari FS, Raman IM (2002) A role for phosphorylation in the maintenance of resurgent sodium current in cerebellar purkinje neurons. *J Neurosci* 22: 3100–3107.
- Hogan B, Beddington F, Costantini F, Lacy E (1994) *Manipulating the Mouse Embryo*. Nashville, Tennessee: Vanderbilt University.
- Russo MJ, Mugnaini E, Martina M (2007) Intrinsic properties and mechanisms of spontaneous firing in mouse cerebellar unipolar brush cells. *J Physiol* 581: 709–724.
- Russo MJ, Yau HJ, Nunzi MG, Mugnaini E, Martina M (2008) Dynamic metabotropic control of intrinsic firing in cerebellar unipolar brush cells. *J Neurophysiol* 100: 3351–3360.
- Rossi DJ, Alford S, Mugnaini E, Slater NT (1995) Properties of transmission at a giant glutamatergic synapse in cerebellum: the mossy fiber-unipolar brush cell synapse. *J Neurophysiol* 74: 24–42.
- Mugnaini E, Sekerkova G, Martina M (2011) The unipolar brush cell: a remarkable neuron finally receiving deserved attention. *Brain Res Rev* 66: 220–245.
- Dino MR, Schuerger RJ, Liu Y, Slater NT, Mugnaini E (2000) Unipolar brush cell: a potential feedforward excitatory interneuron of the cerebellum. *Neuroscience* 98: 625–636.
- Nunzi MG, Mugnaini E (2000) Unipolar brush cell axons form a large system of intrinsic mossy fibers in the postnatal vestibulocerebellum. *J Comp Neurol* 422: 55–65.
- Nunzi MG, Shigemoto R, Mugnaini E (2002) Differential expression of calcitonin and metabotropic glutamate receptor mGluR1alpha defines subsets of unipolar brush cells in mouse cerebellum. *J Comp Neurol* 451: 189–199.
- Sekerkova G, Watanabe M, Martina M, Mugnaini E (2014) Differential distribution of phospholipase C beta isoforms and diacylglycerol kinase-beta in rodents cerebella corroborates the division of unipolar brush cells into two major subtypes. *Brain Struct Funct* 219: 719–749.
- Diana MA, Otsu Y, Maton G, Collin T, Chat M, et al. (2007) T-type and L-type Ca<sup>2+</sup> conductances define and encode the bimodal firing pattern of vestibulocerebellar unipolar brush cells. *J Neurosci* 27: 3823–3838.
- Lein ES, Hawrylycz MJ, Ao N, Ayres M, Bensinger A, et al. (2007) Genome-wide atlas of gene expression in the adult mouse brain. *Nature* 445: 168–176.
- Ruigrok TJ, Hensbroek RA, Simpson JI (2011) Spontaneous activity signatures of morphologically identified interneurons in the vestibulocerebellum. *J Neurosci* 31: 712–724.
- Durmagel S, Kuhn A, Tsiairis CD, Williamson M, Kalbacher H, et al. (2010) Three homologous subunits form a high affinity peptide-gated ion channel in Hydra. *J Biol Chem* 285: 11958–11965.